A new stoichiometry of cuprate nanowires

2012 Supercond. Sci. Technol. 25 115005

(http://iopscience.iop.org/0953-2048/25/11/115005)

Supercond. Sci. Technol. **25** (2012) 115005 (6pp) doi:10.1088/0953-2048/25/11/115005

A new stoichiometry of cuprate nanowires

Joshua Konne[1], Sean A Davis[1], Stefan Glatzel[2], Martin R Lees[3] and Simon R Hall[1]

[1] Complex Functional Materials Group, School of Chemistry, University of Bristol, Cantock's Close, Bristol BS8 1TS, UK
[2] Max Planck Institute of Colloids and Interfaces, Am Mühlenberg 1, D-14476 Potsdam, Germany
[3] Superconductivity and Magnetism Group, Physics Department, University of Warwick, Coventry CV4 7AL, UK

E-mail: simon.hall@bristol.ac.uk

Received 20 July 2012, in final form 31 August 2012
Published 13 September 2012
Online at stacks.iop.org/SUST/25/115005

Abstract
The recent success of making metal oxide nanowires via biopolymer-mediated, sol–gel techniques has been extended to $Y_3Ba_5Cu_8O_{18}$ (Y358), a new cuprate superconductor. This study was carried out using three long chain biopolymers as templates, namely alginate, dextran and chitosan. X-ray diffraction showed an over-expression of the crystallographic *a* axis for samples synthesized in the presence of alginate. The critical current densities (J_c) of Y358 synthesized at 920 °C were 5.01 MA cm^{-2}, 6.26 MA cm^{-2} and 1.24 MA cm^{-2} for alginate, dextran and chitosan respectively.

(Some figures may appear in colour only in the online journal)

1. Introduction

The discovery of high transition temperatures in cuprates created new opportunities for applications of superconductors at temperatures above liquid helium [1–4]. Among the cuprates, yttrium barium copper oxide, $YBa_2Cu_3O_{7-\delta}$ (Y123) has a relatively high critical temperature (T_c) of 93 K and more importantly, has been shown to be able to form anisotropic crystallites and even nanowires with artificial flux pinning centres when synthesized using appropriate conditions and templates [5, 6]. An anisotropic crystal morphology that reduces grain boundary defects and/or disorientations should lead to the enhancement of critical current densities (J_c), necessary for commercial applications of Y123 [7–10]. Superconductivity in the cuprates is considered to be as a result of the motion of charge carriers within the two CuO_2 planes or layers, with the yttrium and barium cations contributing to structural stabilization, doping or creation of holes in the planes. In addition oxygenation of the connecting CuO chains also enhances doping of the planes [11]. T_c has been observed to peak at optimum doping of $\delta \sim 0.16$ and maximum number (n) of CuO_2 planes, $n = 3$ [12, 13]. However, the recent discovery of $Y_3Ba_5Cu_8O_{18}$ (Y358) with five CuO_2 planes and a reported onset T_c of 102 K [14] would suggest an increase in the superconductivity of cuprates with $n > 3$ rather than a decline as earlier predicted. Y358 can be thought of however as an arrangement of a two-plane and three-plane grouping separated by insulating layers, thereby still conforming to the 'n not greater than three' criterion. Like Y123, morphological engineering of Y358 may prove fruitful in order to reduce mis-aligned grain boundaries, thereby making it more amenable for applications. Solid state reaction (SSR), melt-powder-melt-growth (MPMG) and even sol–gel methods have been reported in the synthesis of Y358, albeit with no control over crystal morphology [15, 16]. In this paper we report on the synthesis of the first superconducting nanowires of Y358 crystallites using our proven biopolymer-mediated technique [6].

2. Experimental details

2.1. Sample preparation

A stock solution of Y358 was prepared from a stoichiometric mixture of yttrium, barium and copper nitrates (Sigma-Aldrich) in the ratio of 3:5:8, stirred and allowed to form a homogeneous blue precursor solution.

2.2. Biopolymer solutions

Alginate and chitosan solutions were prepared using the methods reported in literature [6, 17]. Similarly a dextran solution was prepared by dissolving 1 g of dextran in 100 ml of water.

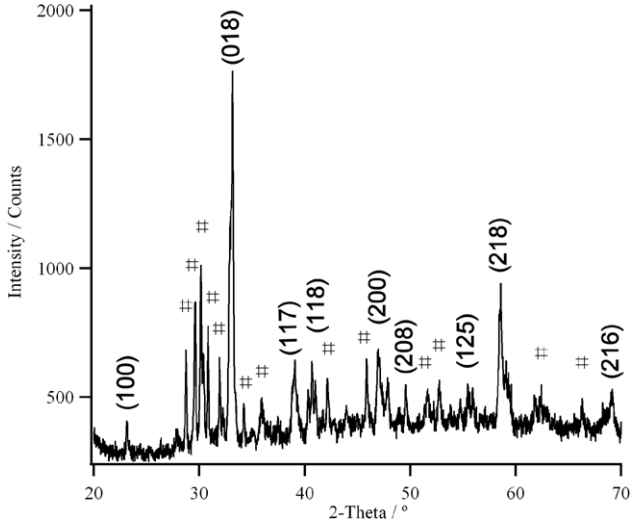

Figure 1. PXRD pattern showing Y358 (indexed) synthesized in the absence of biopolymers. Peaks due to the $BaCuO_2$ impurity phase are marked with #. Y358 peaks are indexed according to the calculated pattern using MAUD, reported in [11].

2.3. Precursor–biopolymer composite

1 ml of Y358 precursor solution was dissolved in 10 ml of each of the biopolymer solutions, stirred to form a light-blue composite gel (alginate) and a homogeneous light-blue liquid (dextran and chitosan) and allowed to dry at 60 °C overnight. The dried composite was calcined at 920 °C for 2 h at a ramp rate of 5 °C min^{-1} in air to form the superconducting phase. Control samples of Y358 without biopolymer were also prepared and calcined at the same heating rate.

2.4. Characterization

The preparation of samples for powder x-ray diffraction (PXRD) was done by grinding a small amount of each sample in an agate mortar with a pestle. The powders were placed on silicon wafers for x-ray diffraction using a Bruker D8 Advance diffractometer. A step size of 0.02 between the scattering angles of 15°–70° was used for all the samples. Scanning electron microscope (SEM) samples were coated with gold and analysed using a JEOL JSM 5600Lv-SEM equipped with an Oxford Instruments energy dispersive x-ray (EDX) detector for analysis. Samples for transmission electron microscopy (TEM) were prepared by placing a drop of a presonicated-aliquot on a carbon coated Ni grid on a filter paper using a Pasteur pipette. The sample was dispersed in ethanol prior to sonication. Dried grids were analysed using a JEOL JEM 1200EX-TEM microscope also equipped with an Oxford Instruments EDX detector for elemental composition analysis. High resolution TEM was carried out using a JEOL JEM 2010 microscope with a similar Oxford Instruments EDX detector. Magnetic susceptibility measurements as a function of temperature were performed using a Quantum Design Magnetic Property Measurement System (MPMS) SQUID magnetometer equipped with a 5 T superconducting magnet under an applied field of 10 mT. Magnetization versus

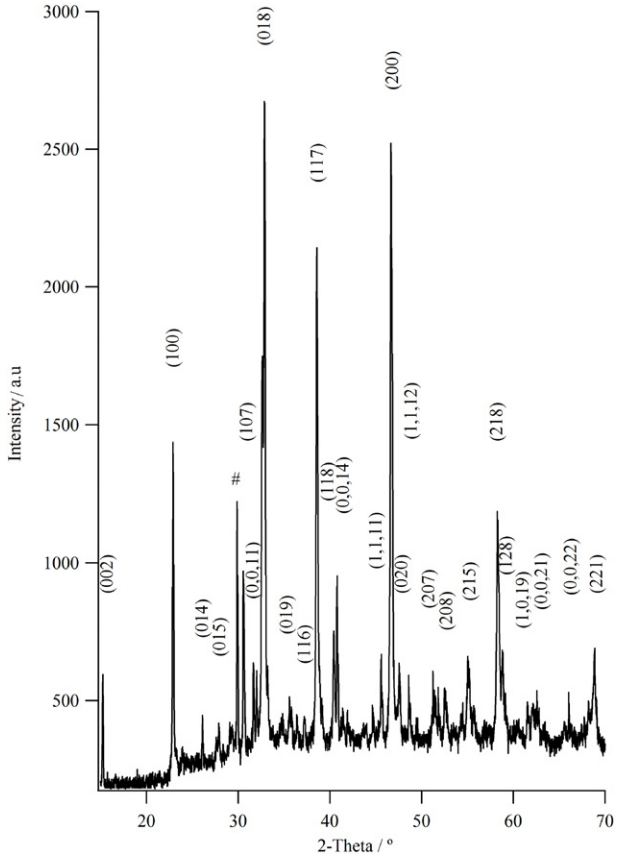

Figure 2. PXRD pattern showing Y358 synthesized in the presence of a biopolymer (alginate). The Y358 phase is indexed, the Y211 impurity peak marked with #.

applied field measurements were also performed at fixed temperature. The intragrain critical current density of the samples was determined by applying a critical state model to full magnetization loops measured at fixed temperatures, assuming a nominal sample density of 6.383 g cm^{-3} and taking the grain (particle) size from the SEM observations. Since such models are known to be inaccurate at low fields (also evident in our data, where the apparent J_c deviates from an exponential field dependence below a certain applied field value), J_c values in the text are stated at applied fields of 1 T.

3. Results and discussion

From figure 1, it can be seen that in the control (no biopolymer) experiment, the Y358 forms as a crystalline material, with a proportion of $BaCuO_2$ as an impurity phase. With the addition of a biopolymer (in this case alginate) to the synthesis however, the formation of $BaCuO_2$ is completely suppressed, with only a small trace of the commonly encountered 'green phase' Y_2BaCuO_5 (Y211 (#)) impurity phase present (figure 2).

The evolution of the superconducting cuprate phase has been shown previously to form at temperatures above 800 °C [17]. In this work therefore, the calcination was monitored using PXRD on each sample collected after quenching the calcination at 10 °C intervals from 800 °C

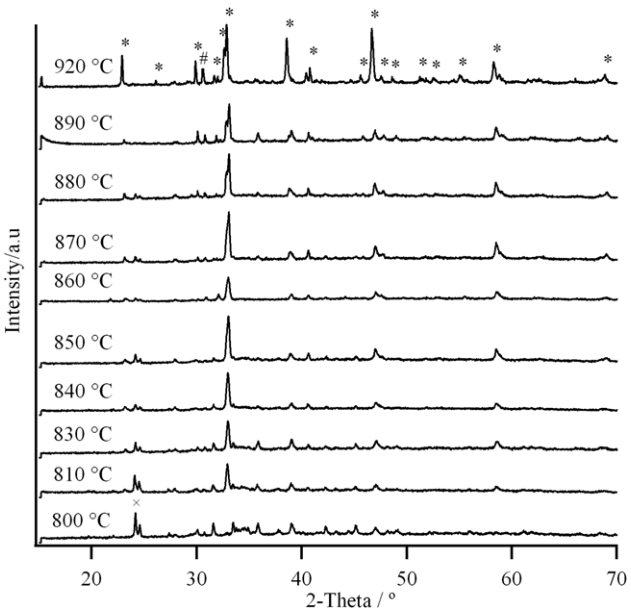

Figure 3. PXRD pattern showing evolution of the Y358 phase (marked with *) and Y211 phase (marked with #). The diminishing barium carbonate peak at 800 °C is marked with an '×'. Y358 peaks are indexed according to the calculated pattern using MAUD, reported in [11].

upwards, until the pure superconducting phase was formed at 890 °C. Alginate was the only biopolymer out of the three studied that could promote the formation of high yields of anisotropic nanorods, therefore this detailed evolution study was limited to the alginate-mediated sample (figure 3). As a general observation, it is clear that the barium carbonate major phase (x) at 800 °C started melting to form the first superconducting phase at 810 °C. Similar evolution studies involving Y123 in an alginate-mediated synthesis [17] showed the emergence of the superconducting phase at 800 °C. This clearly shows that the formation of Y123 and Y358 are following similar thermodynamic pathways. Most strikingly though, it can be seen from the PXRD data that the relative intensities of the crystallographic a reflections are altered significantly in the alginate-mediated Y358 samples over that of the control. Taking the relative intensities ($I/I_o = 100$) where I_o is the intensity of the maximal peak, shows that in the control Y358 (figure 1) the reflections from the lattice planes (018) = 100; (100) = 11; (200) = 23 and (117) = 23. Contrast this with the XRD pattern of alginate-mediated Y358 (figure 2) where relative intensities were observed to be (018) = 100; (100) = 52; (200) = 92 and (117) = 77. These data are indicative of an anisotropic crystalline material with a-axis faces over expressed.

The macromorphology of the Y358 samples was determined using electron microscopy. Impurity phases can be seen as scattered bright spots on top of the porous undulating crystallite sheet in the SEM image of the Y358 control sample (figure 4).

With the introduction of a biopolymer into the synthesis, the macromorphology changed markedly, according to which biopolymer was used. In the case of dextran (figure 5(a)), the Y358 formed a reticulated network, similar to that observed in the control. For chitosan (figure 5(b)), there were a number of anisotropic crystallites formed, albeit these were embedded within a porous matrix. In the case of alginate however,

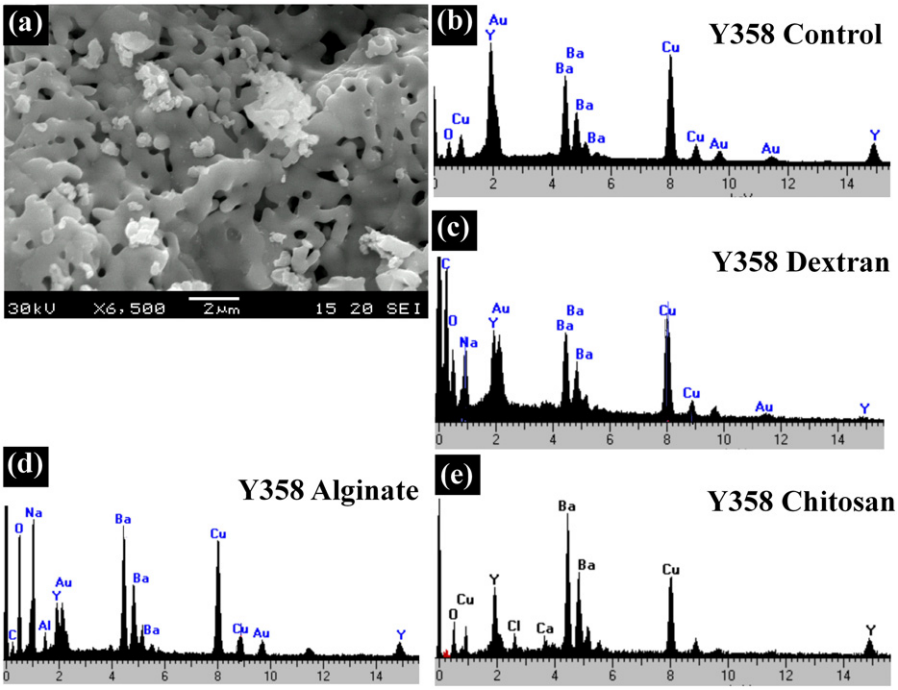

Figure 4. (a) SEM image showing crystallites of the Y358 control sample with (b) corresponding EDX. Spectra for (c) dextran-, (d) alginate- and (e) chitosan-mediated Y358 are also shown.

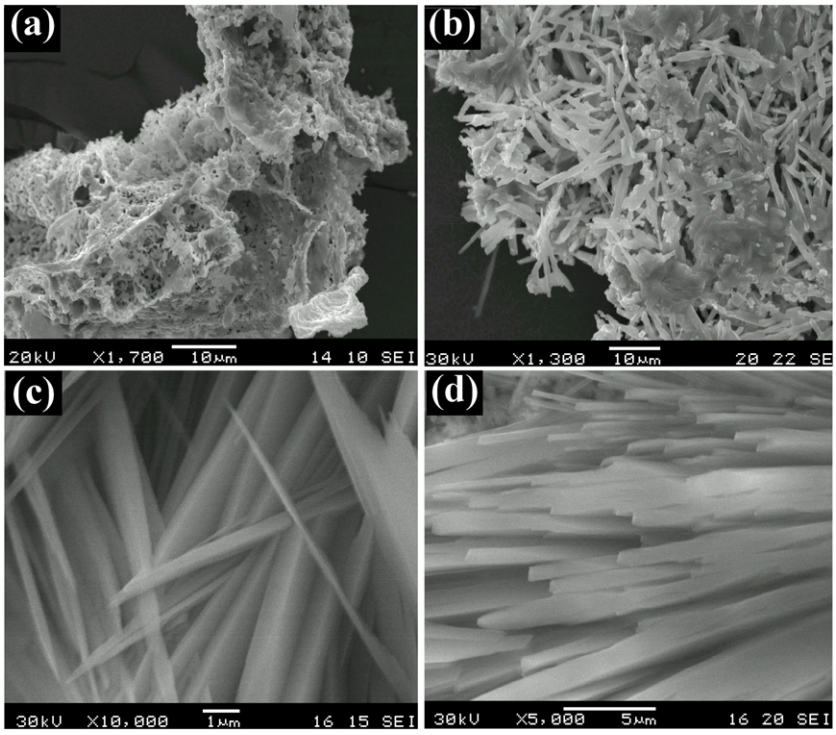

Figure 5. SEM images showing Y358 synthesized in the presence of (a) dextran, (b) chitosan, (c) and (d) alginate.

high yields of highly anisotropic crystallites were produced (figures 5(c) and (d)). The pH values of the solutions of dextran, alginate and chitosan were 6.79, 6.55 and 4.12 respectively. The low pH value for chitosan, the most acidic of the three, was due to the presence of the acidic Cl^- anion. The presence of a Na peak on the EDX spectrum of both anisotropic dextran-mediated and alginate-mediated Y358 products (figures 4(c) and (d)), suggest that Na ions are involved in some way as morphological-directing agents and are not merely 'passive' ions.

From figure 4, it can be seen that the presence of sodium was strongest in association with the alginate-mediated samples than in either of the other systems investigated. The sodium in the alginate comes from the sodium bicarbonate used in the acidification stage of sodium alginate processing. In terms of a mechanism, it is possible that sodium atoms are acting to lower the temperature of flux formation locally, leading to an earlier melting transition of barium carbonate at temperatures less than 800 °C and subsequent catalytic outgrowth of the anisotropic Y358 morphology. The formation of a lower-melting sodium carbonate/barium carbonate eutectic is currently the subject of further investigation, as its role in the melting of $BaCO_3$ nanoparticles of the pre-ceramic crystalline phase, which subsequently act as catalytic sites for the spatial outgrowth of nanowires has been postulated previously [17, 18]. That sodium is also present in dextran, yet no anisotropic morphology results from the synthesis, highlights the additional role of molecular configuration in the pre-ordering of metal cations. Dextran is a hyper-branched polysaccharide, with a random spatial distribution of cationic chelating sites and as a result, the formation of barium carbonate is not restricted to well-dispersed sites. This leads to the formation of larger crystallites of $BaCO_3$, thereby rendering them incapable of fully melting during the course of the calcination and being unavailable for catalytic outgrowth of nanowires. Contrast this with the highly regular domains in alginate where chelation is strong (the so-called 'egg-box' model of cation binding [19]), which naturally restricts the formation of barium carbonate to discrete sites of nucleation and growth. The resultant phase is therefore nanoparticulate and is able to melt fully and allow the formation of stoichiometric Y358 nanowires by the end of calcination.

High resolution TEM of one of the alginate-mediated Y358 nanowires is shown in figure 6(a). This clearly shows the lattice fringes of the crystallite, confirming the phase. The fast Fourier transform (FFT) showing the (018) lattice planes of this region is inset. The TEM micrographs and SAED patterns (inset) of chitosan- and dextran-mediated samples are shown in figures 6(b) and (c) respectively. Both were able to be indexed to Y358. The alginate-mediated samples showed more crystallites grown with the crystallographic *a*-axis over expressed, confirming the anisotropic morphology.

SQUID magnetometry of all the samples showed that the alginate-mediated Y358 synthesized at 890 °C had a high J_c of 7.26 MA cm^{-2} at 10 K (figure 7(a)) and a T_c of 89.4 K (measured in an applied field of 1 T). Further calcinations possibly increased the oxygen content causing a slight decrease in the T_c and J_c of the 920 °C sample to 88 K and 5.01 MA cm^{-2} (figure 7(b)) respectively. The dextran-mediated (figure 7(c)) sample produced a J_c of 6.26 MA cm^{-2} and the highest T_c of 90 K. The superconducting volume of the dextran-mediated sample however, was approximately half that of the alginate-mediated sample. The critical current

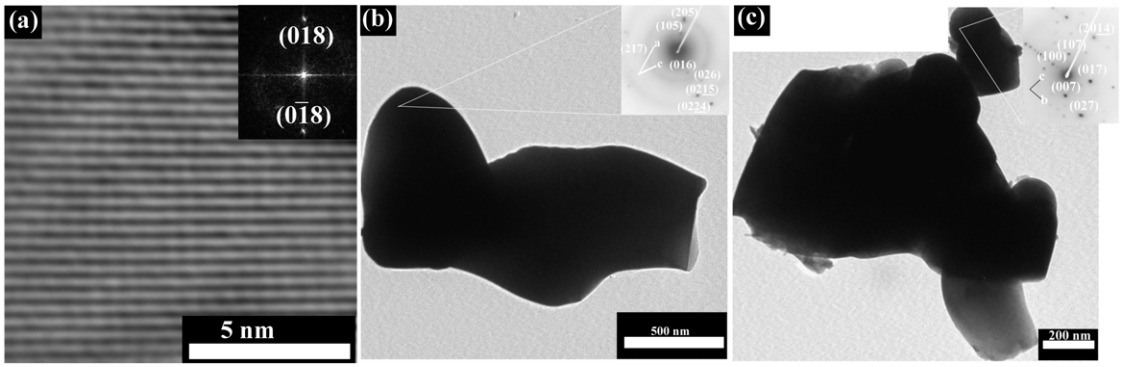

Figure 6. HR-TEM images of (a) the surface of a Y358 nanowire grown in an alginate-mediated synthesis, showing lattice fringes and (b) Y358 chitosan-mediated and (c) Y358 dextran-mediated samples respectively. Indexed FFT is inset in (a) and SAED of each crystallite is inset in (b) and (c).

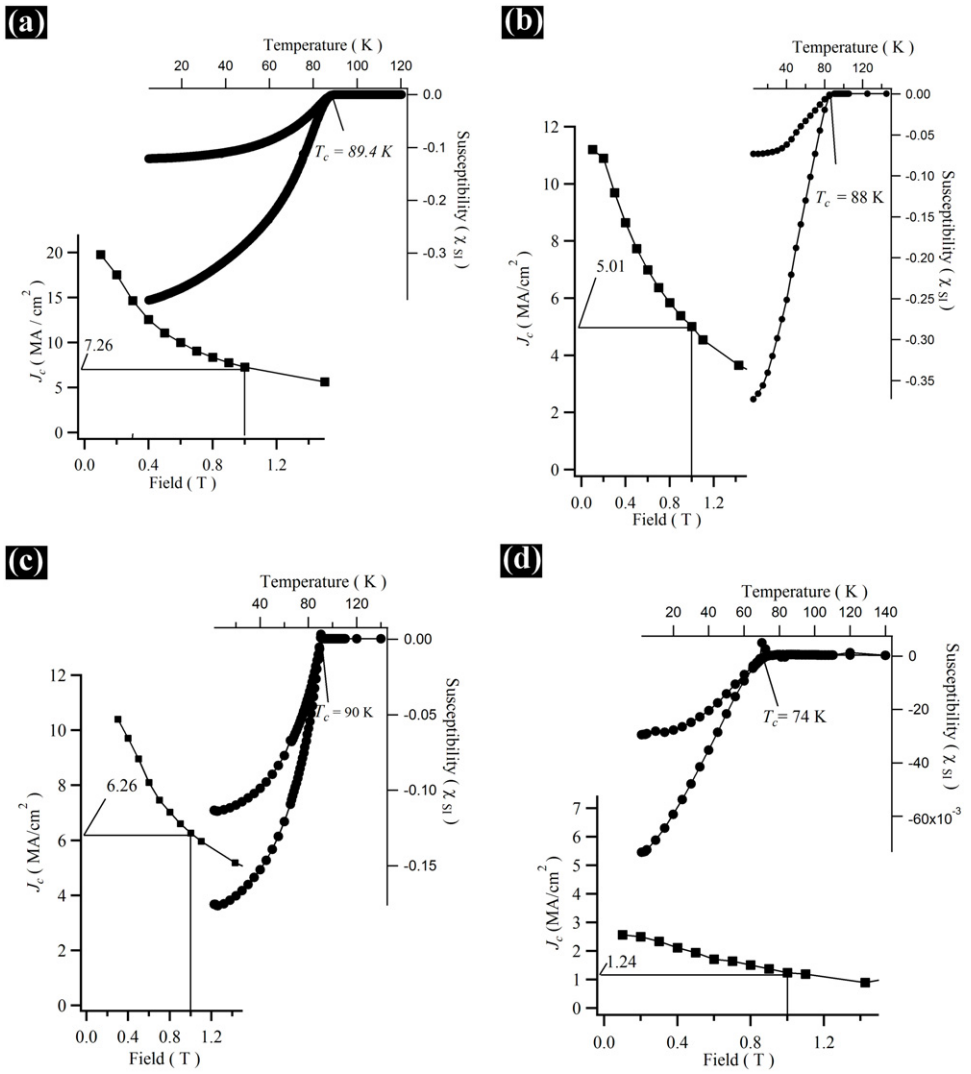

Figure 7. SQUID data from (a) 890 °C alginate-mediated, (b) 920 °C alginate-mediated, (c) dextran-mediated and (d) chitosan-mediated Y358 samples respectively.

density of both samples compare very favourably to cuprate nanowires synthesized previously [17] which had a critical temperature of 77 K and J_c of 2.42 MA cm^{-2} at 10 K and 1 T of applied field. Clearly the Y358 stoichiometry shows improved superconducting properties over that reported previously for cuprate nanowires.

The pinning of vortices by defects due to the presence of impurities in the lattice of superconductors has been known

to increase J_c, and so the presence of metal cations from the biopolymers may be contributory factors to the high J_c values for alginate- and dextran-mediated Y358. The relatively low J_c value for chitosan-mediated Y358 could be a result of the presence of chlorine preventing calcium from interacting with the superconducting phase, through the formation of amorphous $CaCl_2$. The T_c of this sample was 74 K, the lowest of the three biopolymer-mediated samples.

The depression of T_c from that expected (approx. 93 K for Y123) in anisotropic high temperature superconductors has been demonstrated previously to be due to phase-slip processes [20, 21], which become more pronounced as the thickness of the nanowire decreases. The difference between the literature onset T_c values for Y358 (approx. 102 K) and the values we present here may possibly be a function of this morphological effect. Previously, it was shown that for 10 nm Y123 nanowires, the superconducting transition was significantly broadened and zero resistance was not reached until very low (approx. 20 K) temperatures were reached [22]. Although still higher than conventional superconductor nanowires, this does not render them any better in terms of cost to application, owing to liquid helium still being required as a cryogen. Whilst more work needs to be done to interrogate the superconducting behaviour of individual nanowires in the system presented here, it is encouraging that magnetic susceptibility is <0 for all of our alginate-mediated Y358 nanowires at liquid nitrogen temperatures. As their widths are not less than 100 nm, according to models, the transition to zero resistance should not be broadened significantly, nor should the T_c be suppressed much below that reported previously for the bulk material.

4. Conclusion

Y358 with an anisotropic morphology and a high critical current density and critical temperature, has been produced for the first time. Synthesis of Y358 using three biopolymers has shown that the best results in terms of yields of nanowires and nanorods can be achieved via an alginate-mediated route. Pre-organization of cations via the egg-box model of ion binding in alginate appears to be key in the anisotropic crystal growth processes during calcination. We have also shown that alginate and dextran biopolymers can dope the superconducting phase with sodium and that these impurities could be acting to increase J_c by introducing additional pinning centres. Further work however needs to be done in order to accurately map the position of Na in relation to the nanowire lattice to gain a deeper understanding about the role of sodium in Y358 nanowire formation.

Acknowledgments

The authors would like to thank the Petroleum Technology Development Fund (PTDF) Abuja, Nigeria for their support in scholarship funding of this research. We would also like to thank the Royal Society for the award of a URF to one of us (SRH) and Mr Jonathan Jones for the High resolution electron microscopy. The magnetometer used in this research was obtained through the Science City Advanced Materials project: Creating and Characterizing Next Generation Advanced Materials project, with support from Advantage West Midlands (AWM) and part funded by the European Regional Development Fund (ERDF).

References

[1] Bednorz J G and Muller K A Z 1986 *J. Phys.: Condens. Matter* **64** 189
[2] Chu C W, Hor P H, Meng R L, Gao Z J, Huang Y Q and Wang Y Q 1987 *Phys. Rev. Lett.* **58** 405
[3] Wu M K, Ashburn J R, Torng C J, Hor P H, Meng R L, Gao Z J, Huang Y Q, Wang A and Chu C W 1987 *Phys. Rev. Lett.* **58** 908
[4] Schilling A, Cantoni M, Guo G D and Ott H R 1993 *Nature* **363** 56
[5] Wimbush S C, Marx W, Barth A and Hall S R 2010 *Supercond. Sci. Technol.* **23** 1
[6] Hall S R 2006 *Adv. Mater.* **18** 487
[7] Larbalestier D, Gurevich A D, Feldmann M and Polyanskii A 2001 *Nature* **414** 368
[8] Hilgenkamp H and Mannhart J 2002 *Rev. Mod. Phys.* **74** 485
[9] Mulet R, Diaz O and Altshuler E 1997 *Supercond. Sci. Technol.* **10** 758
[10] Klie R F, Buban J P, Varela M, Franceschetti A, Jooss C, Zhu Y, Browning N D, Pantelides S T and Pennycook S J 2005 *Nature* **435** 475
[11] Aliabadi A, Farshchi Y A and Akhavan M 2009 *Physica* C **469** 2012
[12] Strickland N M, Semwal A, Williams G V M, Verebelyi D T and Zhang W 2004 *Supercond. Sci. Technol.* **17** S473
[13] Pickett W E 2006 *Iran. J. Phys. Res.* **6** 29
[14] Tavana A and Akhavan M 2010 *Eur. Phys. J.* B **73** 79
[15] Bolat S and Kutuk S J 2012 *J. Supercond. Novel Magn.* **25** 731
[16] Ekicibil A, Cetin S K, Ayas A O, Coskun A, Firat T and Kiymac K 2011 *Solid State Sci.* **13** 1954
[17] Schnepp Z A C, Mann S, Wimbush S C and Hall S R 2008 *Adv. Mater.* **20** 1782
[18] Schnepp Z A C, Wimbush S C, Mann S and Hall S R 2010 *CrystEngCommun.* **12** 1410
[19] Morris E R 1986 *Br. Polym. J.* **18** 14
[20] Lau C N, Markovic N, Bockrath M, Bezryadin A and Tinkham M 2001 *Phys. Rev. Lett.* **87** 217003
[21] Tinkham M 1996 *Introduction to Superconductivity* 2nd edn (New York: McGraw-Hill)
[22] Xu K and Heath J R 2008 *Nano Lett.* **8** 3845